

# The Use of Chlorobenzene as a Probe Molecule in Molecular Dynamics Simulations

Yaw Sing Tan,<sup>†,‡</sup> David R. Spring,<sup>†</sup> Chris Abell,<sup>†</sup> and Chandra Verma<sup>\*,‡,§,⊥</sup>

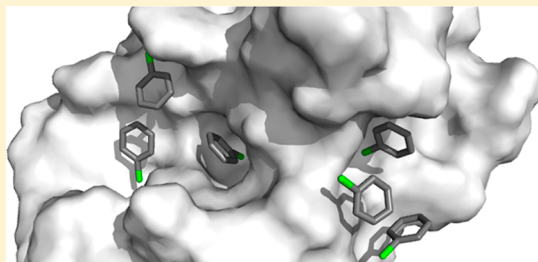
<sup>†</sup>Department of Chemistry, University of Cambridge, Lensfield Road, Cambridge CB2 1EW, United Kingdom

<sup>‡</sup>Bioinformatics Institute (A\*STAR), 30 Biopolis Street, #07-01 Matrix, Singapore 138671

<sup>§</sup>Department of Biological Sciences, National University of Singapore, 14 Science Drive 4, Singapore 117543

<sup>⊥</sup>School of Biological Sciences, Nanyang Technological University, 60 Nanyang Drive, Singapore 637551

## Supporting Information



**ABSTRACT:** We map ligand binding sites on protein surfaces in molecular dynamics simulations using chlorobenzene as a probe molecule. The method was validated on four proteins. Two types of affinity maps that identified halogen and hydrophobic binding sites on proteins were obtained. Our method could prove useful for the discovery and development of halogenated inhibitors.

## INTRODUCTION

Halogens, especially fluorine and chlorine, are common substituents used in drug design<sup>1</sup> to enhance binding affinity and improve pharmacokinetic properties, such as oral absorption<sup>2</sup> and blood-brain barrier permeability.<sup>3</sup> Binding affinity improvements conferred by halogenation have been attributed traditionally to favorable van der Waals interactions with the target protein and, more recently, to the formation of halogen bonds, which are highly analogous to hydrogen bonds in terms of strength and directionality.<sup>4</sup> Halogen bonding is driven by the  $\sigma$ -hole,<sup>5</sup> which is a positively charged region on the outermost part of the halogen atom along the covalent-bond axis. Organofluorines generally do not have a  $\sigma$ -hole due to the high electronegativity and low polarizability of the fluorine atom,<sup>6</sup> and so only the heavy organohalogens (organochlorines, organobromines and organoiodines) are able to form halogen bonds. Two types of halogen bonds have been observed: one involving interactions with a Lewis base and one involving interactions with  $\pi$ -surfaces. Within a protein, a ligand not only can form halogen bonds with the backbone carbonyl oxygens, but also side chain groups such as hydroxyl oxygens in serine, threonine, and tyrosine, carboxylate oxygens in aspartate and glutamate, amide oxygens in asparagine and glutamine, sulfurs in cysteine and methionine, nitrogens in histidine, and the aromatic surfaces of phenyl-

alanine, tyrosine, tryptophan, and histidine.<sup>7</sup> The ability of halogens to engage in such a multitude of ligand–protein interactions renders them very useful in rational drug design where several successful case studies have been reported.<sup>8–10</sup>

The multiple solvent crystal structure (MSCS) method<sup>11</sup> is a fragment-based experimental technique that uses organic solvents as probes to map ligand binding sites on proteins. X-ray crystal structures of a target protein are resolved in the presence of various organic solvents, allowing for the location and characterization of solvent binding sites that can then be manipulated as putative ligand binding sites. Such experimental approaches require significant investment of time, energy, and effort. Computational methods have the potential to mitigate such costs considerably. Early efforts to develop computational methods that predict binding sites include the GRID program by Goodford<sup>12</sup> and the multiple copy simultaneous search (MCSS) approach,<sup>13</sup> neither of which account for protein flexibility and require the binding sites to be already accessible on the input protein structure. The computational analogue of MSCS is the FTMap method,<sup>14</sup> which can be applied to ensembles of protein structures generated by molecular dynamics (MD) simulations.<sup>15</sup> While this incorporates the flexibility of the apo protein, it is still limited by the absence of both ligand and ligand-induced protein flexibility during mapping. To overcome this limitation and also to better describe solvation effects, there have been recent efforts to develop methods that incorporate the concept of MSCS into explicit-solvent MD simulations. Ligands selected based on their drug-like features and prevalence as substructures in drug molecules are introduced into protein–solvent systems to probe protein surfaces, yielding ligand affinity maps.<sup>16–21</sup> To date, the use of aromatic, aliphatic, hydrogen-bond donor, hydrogen-bond acceptor, and charged ligands as probe molecules in these approaches has been described; however, there has been no reported use of halogenated ligands as probes.

In this study, we propose the use of chlorobenzene as a probe molecule in MD simulations. We have previously described the ligand-mapping simulation technique, in which benzene molecules were used as probes to successfully design a ligand to target a protein–protein interaction.<sup>20</sup> Considering the increasing importance of halogens in drug development, the

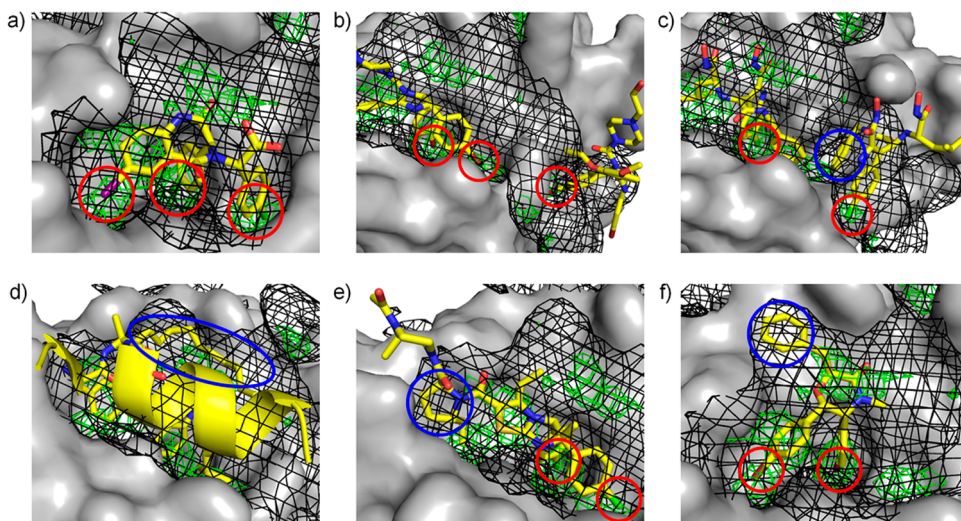


**Figure 1.** Chlorobenzene occupancy maps (green mesh for chlorine atoms, black mesh for carbon atoms) overlaid on crystal structures of MDM2 complexes with (a) a benzodiazepinedione inhibitor (PDB 1T4E), (b) nutlin-2 (PDB 1RV1), (c) a 6-chloroindole inhibitor (PDB 4MDQ), (d) an *i*, *i*+7 stapled peptide (PDB 3V3B), (e) a dihydroimidazothiazole inhibitor (PDB 3W69), and (f) a morpholinone inhibitor (PDB 4JV7). Areas of overlap between the chlorine occupancy maps and ligand halogen atoms are circled in red, while areas of overlap between the carbon occupancy maps and hydrophobic moieties are circled in blue.

ligand-mapping method was refined to probe for both aromatic and halogen interaction sites. Four proteins, for which structural data on halogenated ligands is available and which exhibit significant conformational changes upon ligand binding, were chosen to validate our enhanced ligand-mapping methodology.

## RESULTS AND DISCUSSION

Halogenation of compounds is commonly used during the drug development process. In particular, chlorine is a moderate halogen-bond acceptor, and the C–Cl bond is relatively stable, which may explain why it is the most prevalent halogen among small-molecule modulators of protein–protein interactions<sup>22</sup> and launched drugs listed in Thomson Reuters Pharma over the last century.<sup>23</sup> In order to explore the sites for halogen interactions, we chose chlorobenzene as the candidate probe so that in addition to chlorine interactions, the phenyl group of chlorobenzene would concurrently also be able to probe for hydrophobic binding sites.

We chose four proteins involved in protein–protein interactions to test the ability of our method to reproduce experimental data: MDM2, MCL-1, interleukin-2, and Bcl-xL. These proteins have available structural data of halogenated ligands in the Protein Data Bank (PDB) and display significant conformational changes on ligand binding. In particular, some (MDM2, MCL-1, Bcl-xL) or all (interleukin-2) of the halogen binding sites are absent in both the unbound states of these proteins as well as when they are bound to their natural protein or peptide partners. The protein structures were specifically extracted from these complexes and used to initiate the ligand-mapping simulations (see Supporting Information for details), thus ensuring a rigorous test of the utility of our method.

Several changes to the protocol were introduced compared to our previous study in which benzene was used as the probe molecule.<sup>20</sup> Simulation conditions were initially refined using MDM2, which has the most extensive structural data of halogenated ligands among the four test proteins, before extending them to the other three proteins. Chlorobenzene was used at a lower concentration of 0.15 M, as compared to 0.2 M

for benzene, since significant aggregation of chlorobenzene was observed at the higher concentration. Such aggregation is undesirable because it lowers the effective ligand concentration and prevents thorough sampling of the protein surface.<sup>17</sup> The lower ligand concentration necessitated an increase in the simulation length to 10 ns from 5 ns used previously, for better sampling. Ligand-induced denaturation of the target protein<sup>24</sup> due to the increased simulation length was not an issue as stable trajectories were observed for all four proteins (Figure S1). Lastly, due to the increased lipophilicity of chlorobenzene compared to benzene, a lower proportion of chlorobenzenes was observed to remain in solution during the simulations. This necessitated the utilization of a higher cutoff isocontour value for visualization of the occupancy grids. This was set at five times the threshold bulk value, which is defined as the highest isovalue at which chlorobenzene carbon or chlorine atoms are respectively detected in the bulk solvent. A comparison of the aromatic carbon occupancy maps of MDM2 generated from benzene-mapping and chlorobenzene-mapping simulations showed that they concurred on the prediction of most hydrophobic binding sites (Figure S2). The nonconsensus sites are not known to bind any ligands. This suggests that chlorobenzene is a suitable replacement for benzene as a probe for hydrophobic binding sites.

**MDM2.** The MDM2–p53 interaction is one of the most studied protein–protein interactions and there is extensive structural data available in the PDB of MDM2 complexes. The protein structure used to initiate the ligand-mapping simulations was obtained from the complex of MDM2 with the p53 transactivation domain peptide (PDB 1YCR).<sup>25</sup>

Together, the various structures of MDM2 available in the PDB suggest that there are at least six halogen binding sites in the N-terminal domain of MDM2. Three of them correspond to the locations of the three p53 hot-spot residues, Phe19, Trp23 and Leu26. These sites are occupied by a benzodiazepinedione inhibitor (PDB 1T4E)<sup>26</sup> and have been successfully mapped by the chlorobenzenes in our study, as shown in Figure 1a. Two other halogen binding sites are found adjacent to the p53 binding cleft. There are two molecules of nutlin-2 in the

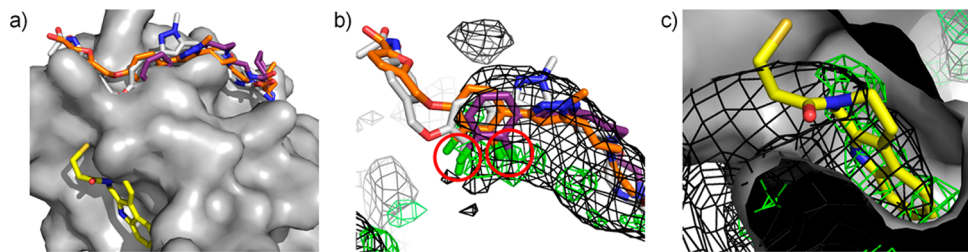


**Figure 2.** Small-molecule binding to IL-2. (a) Small molecules from IL-2 complexes superimposed on IL-2 structure used for ligand-mapping simulations reveal two cryptic binding sites. Chlorobenzene occupancy maps (green mesh for chlorine atoms, black mesh for carbon atoms) overlaid on crystal structures of IL-2 complexes with (b) dichlorinated compounds (PDB 1PW6, 1PY2, 1QVN), and (c) a covalently tethered small-molecule ligand (PDB 1NBP). Areas of overlap between the chlorine occupancy maps and ligand halogen atoms are circled in red.

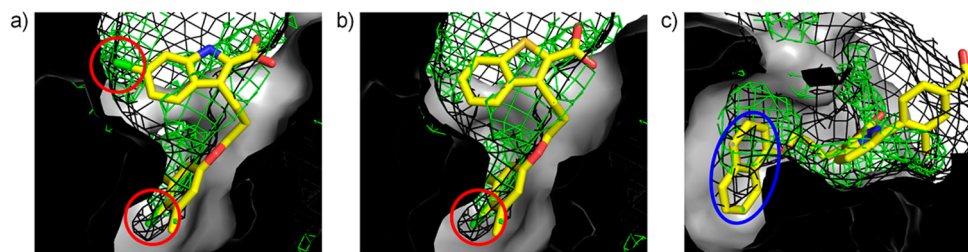


**Figure 3.** Chlorobenzene occupancy maps (green mesh for chlorine atoms, black mesh for carbon atoms) overlaid on crystal structures of MCL-1 complexes with (a) a dichlorinated compound (PDB 4HW2), (b) monochlorinated compound (PDB 4HW3), and (c) a pyrazolo[1,5-a]pyridine derivative (PDB 3WYI). Areas of overlap between the chlorine occupancy maps and ligand halogen atoms are circled in red, while the blue circle highlights a pocket that is not occupied by BH3 peptide binders of MCL-1.

structure of an MDM2/nutlin-2 complex (PDB 1RV1),<sup>27</sup> as shown in Figure 1b. One molecule is bound to the main p53 binding site, and the other is bound, through one of its bromophenyl moieties, to a second nutlin interaction site; this site is occluded in the initial MDM2 structure. The chlorine densities coincide with the location of the bromine atom of the latter nutlin molecule, indicating a halogen binding site. This is stabilized by a halogen bond with the carbonyl oxygen of Tyr100. This second nutlin interaction site was also mapped by the carbon atoms of the chlorobenzene probes, indicating that it might be a potential druggable site that could be explored for ligand binding. The fifth detected halogen binding site is adjacent to the second nutlin interaction site. Similar to the observation of two nutlin binding sites in the MDM2/nutlin-2 complex structure, two chloroindole-based inhibitor molecules are complexed to MDM2 in the crystal structure of the complex (PDB 4MDQ).<sup>28</sup> One is bound at the main binding cleft, while the second molecule is bound at a site between the two nutlin interaction sites (Figure 1c). The locations of the phenyl and chloroindole groups of the second molecule were recapitulated by the chlorobenzene occupancy maps. The sixth halogen binding site is found in the vicinity of this ‘intermediate site’ and is formed partially by residues 17–24 of MDM2 (PDB 4MDN).<sup>28</sup> These N-terminal residues were absent in our input MDM2 structure and could explain why this last halogen binding site was not detected by the chlorobenzenes. An additional set of chlorobenzene-mapping simulations was initiated using this MDM2 structure to see if the last halogen binding site could be detected in the presence of a longer N-terminal tail. The chlorobenzene map generated showed distinct chlorine density close to the chloro substituent of the ligand in the 4MDN structure (Figure S3), suggesting that a more complete MDM2 structure was indeed necessary for successful (i.e., more accurate) detection of this halogen binding site.

Besides mapping halogen binding sites, the chlorobenzenes also found hydrophobic sites, even those that require significant protein conformational changes. A total of four such cryptic hydrophobic binding sites, which are not present in the initial MDM2 structure, were identified in the ligand-mapping simulations. The ‘intermediate site’ mentioned earlier is an extension of the Leu26 binding site (Figure 1c) and is one of the cryptic hydrophobic sites revealed by the chlorobenzene probes. Similarly, although the binding site for the hydrocarbon staple of an *i, i + 7* stapled peptide (PDB 3V3B)<sup>29</sup> was not visible in the initial protein structure, the chlorobenzenes were able to successfully map it. (Figure 1d). In Figure 1e, the pyrrolidine moiety of the inhibitor (PDB 3W69)<sup>30</sup> pushes against the walls of the Phe19 binding site, creating another hydrophobic interaction site by induced-fitting. Finally, in Figure 1f, the benzyl group of a morpholinone inhibitor (PDB 4JV7)<sup>31</sup> engages in an edge-face  $\pi-\pi$  interaction with Phe55 on a shallow hydrophobic binding region that is obscured by side chains in the input structure.

**Interleukin-2.** The cytokine protein interleukin-2 (IL-2) binds to the IL-2 receptor (IL-2R) to induce T-cell proliferation.<sup>32</sup> Small molecules have been shown to bind at two adaptive cryptic sites on IL-2 that are not apparent in the apo, IL-2/IL-2R $\alpha$ , and the complete IL-2/IL-2R complex structures (Figure 2a).<sup>33–36</sup> These two sites have been studied by a fragment-based MD technique and shown to reveal themselves in the presence of a highly concentrated solution of benzenes and propanes.<sup>24</sup> Similarly, we have mapped these two pockets with chlorobenzene probes, as shown by the aromatic carbon densities in Figure 2b,c. In addition, the chlorine densities coincide with the positions of two chlorine substituents in chlorinated IL-2 inhibitors (Figure 2b). There is good overlap between the carbon densities at the pyrazole ‘arm’ of the inhibitors (right of Figure 2b), but there are no carbon densities at the other end of two of the inhibitors.

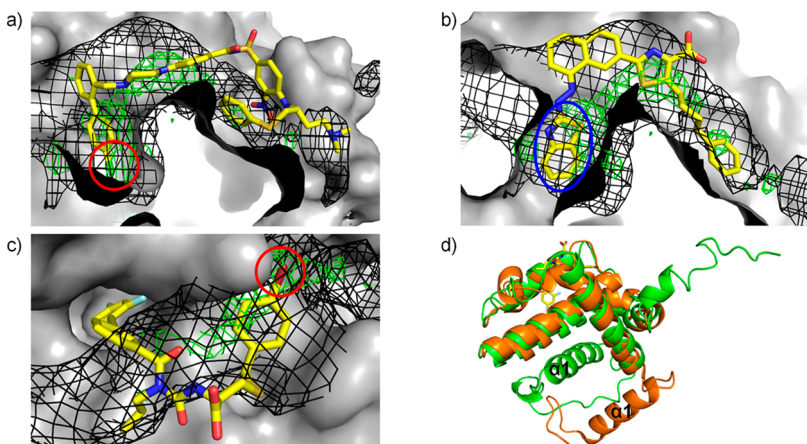


**Figure 4.** Chlorobenzene occupancy maps (green mesh for chlorine atoms, black mesh for carbon atoms) overlaid on crystal structures of Bcl-xL complexes with (a) a chlorinated inhibitor (PDB 2YXJ), (b) a benzothiazole inhibitor (PDB 3ZLO), and (c) a benzoylurea inhibitor (PDB 4CSD). Areas of overlap between the chlorine occupancy maps and ligand halogen atoms are circled in red, while the blue circle highlights a pocket that is not occupied by BH3 peptide partners of Bcl-xL. (d) Comparison of the position of helix  $\alpha$ 1 in monomeric (green) and dimeric (orange) Bcl-xL, with the benzoylurea inhibitor (yellow sticks) superimposed (PDB 4CSD).

Experimental data have shown that binding affinity was enhanced when a furoic acid fragment was added, but not when it was replaced with a neutral phenylacetamide group.<sup>36</sup> This suggests that the extension provides only favorable electrostatic interactions and does not actually occupy a particular hydrophobic binding site, which is in agreement with the lack of carbon density in the region.

**MCL-1.** MCL-1 is an antiapoptotic protein that suppresses apoptosis by sequestering the pro-apoptotic Bcl-2 family proteins<sup>37</sup> and is found to be overexpressed in a variety of human cancers.<sup>38–40</sup> It contains a hydrophobic binding groove that binds the BH3  $\alpha$ -helices of these proteins. BH3 helix mimicry has been the basis for the development of MCL-1 inhibitors to sensitize cancer cell apoptosis for anticancer therapy.<sup>41</sup> Such efforts have led to the development of small molecules that bind at the BH3 binding pocket and three of them are shown in Figure 3.

The crystal structure of MCL-1 bound to a dichlorinated compound (Figure 3a) shows that there are at least two halogen interaction sites within the binding cavity,<sup>42</sup> the deeper of which is occluded in the starting MCL-1 conformation derived from an MCL-1/Bim BH3 peptide complex structure (PDB 3KJ0). Both sites were successfully detected in the ligand-mapping simulations. One of the chlorines forms a halogen bond with the carbonyl oxygen of Ala227, whereas the other chlorine found at the lower part of the pocket engages in purely van der Waals interactions with the protein (Figure 3b). The occupancy maps also indicated chlorine density at one of the meta-positions of the chlorinated phenyl group (Figure 3a,b). This points to a possible halogen binding site, where a halogen bond could be formed with the carbonyl oxygen of the nearby Leu246.

The BH3 binding pocket of MCL-1 is very deep, but its full capacity is not utilized by the BH3 peptides. The full depth of the pocket has been explored by small molecules, however, as shown by the 4-chloro-3,5-dimethylphenyl groups of the ligands in Figure 3a,b and the naphthyl group of the ligand in Figure 3c. Significant protein backbone movements are required for the accommodation of these hydrophobic moieties,<sup>42,43</sup> but this does not prevent the chlorobenzene

probes from inducing these changes and reproducing the ligand interactions at the bottom of the pocket.

**Bcl-xL.** Like MCL-1, Bcl-xL is an antiapoptotic protein that neutralizes proapoptotic proteins such as Bax and Bak by binding to their  $\alpha$ -helical BH3 domains. It is frequently overexpressed in cancer cells, leading to chemotherapy resistance.<sup>44,45</sup> The use of BH3 mimetics to inhibit its interactions with proapoptotic proteins is therefore of great interest in cancer therapy.<sup>41</sup>

There are two large binding pockets in Bcl-xL, as shown in Figure 4a. The deeper and more well-defined pocket is occupied by the 4-chlorophenyl group of the ligand, while the shallower pocket is occupied by a thiophenol group. The chlorine interaction site in the deep pocket is occluded in the apo structures<sup>46–48</sup> as well as in the structure of the complex with the Bak peptide (PDB 1BXL) that was used as the initial structure for the ligand-mapping simulations. Nevertheless, this interaction was detected by the chlorobenzene probes, as the chlorine densities derived from the simulations coincide with the position of the chlorine atom in the 4-chlorophenyl group (Figure 4a). Another chlorine interaction site was identified in the shallow pocket, near the meta-position of the phenyl group. Currently, there is no structural data showing ligands engaging the shallow pocket with halogenated groups. Known Bcl-xL inhibitors having a similar binding mode as the ligand in Figure 4a could be modified to present a 3-chlorophenyl group at the shallow pocket to enhance their binding affinities.

The compound in Figure 4b is bound to a different Bcl-xL conformation from that in Figure 4a but engages the same binding pockets. The benzothiazole group of the compound is shown fully utilizing the capacity of the deeper Bcl-xL pocket, just like the 4-chlorophenyl group in Figure 4a. Although the location of these two hydrophobic moieties in Bcl-xL was occluded in the starting structure used for the ligand-mapping simulations, chlorobenzene probes were able to expose them by inducing side chain movements to expand the pocket, as evidenced by the presence of carbon densities deep in the pocket.

Recent crystal structures of Bcl-xL complexes reported by Brady et al.<sup>49</sup> show the difluorophenyl groups of two benzoylurea inhibitors projecting into a previously unreported

pocket near the BH3 binding groove (Figure 4c). This hydrophobic pocket was not detected in the ligand-mapping simulations; however, another halogen interaction site in Bcl-xL, as indicated by the bromophenyl group of the benzoylurea inhibitor, was detected by the chlorobenzene probes. The structure of Bcl-xL in one of the crystal structures obtained by Brady et al. was compared to the Bcl-xL solution structure used for the simulations (Figure 4d). The most striking difference was in the position of helix  $\alpha$ 1, which was seen to undergo a significant conformational change between the two structures. Bcl-xL exists as a dimer in the newly reported crystal structures. On dimerization, a domain swap involving helix  $\alpha$ 1 occurs between the monomers. The original position of  $\alpha$ 1 is occupied by the helix  $\alpha$ 1 from another protein chain. This could possibly have altered the dynamics of the Bcl-xL subunit significantly enough to allow the opening of this cryptic pocket, which would otherwise remain closed in the monomeric state, thus explaining why it was not detected in the ligand-mapping simulations.

## CONCLUSION

We have described a reliable method of mapping halogen and hydrophobic binding sites on protein surfaces by incorporation of chlorobenzene molecules into MD simulations. This is an evolution of our previous implementation of ligand-mapping simulations that used benzene probes,<sup>20</sup> since two types of affinity maps can now be obtained in a single set of simulations. We have also demonstrated that the chlorobenzene probes are able to expose binding sites that are occluded in the input structures of four proteins involved in protein–protein interactions. Such sites are of utmost importance in the design of small molecule inhibitors of protein–protein interactions, as the target protein may appear flat and undruggable even when bound to its protein or peptide partner.<sup>50</sup> The ensemble of simulated protein conformations with these cryptic sites exposed may then be used for small molecule docking in structure-based virtual screening. Additionally, affinity maps obtained from ligand-mapping simulations could be used to guide the elaboration of fragments and hit compounds, by revealing favorable sites for the addition of halogens and hydrophobic groups.

The ability of the method to reproduce known halogen binding sites in our test set of proteins is rather remarkable, taking into consideration the inaccuracies of the force field used to describe halogen bonding between chlorobenzene probes and the protein. Like all other classical force fields used in biomolecular modeling, the general AMBER force field (GAFF)<sup>51</sup> assigns isotropic partial charges to atoms and does not account for the anisotropic distribution of the electrostatic potential on halogen atoms. Halogen atoms are usually assigned negative partial charges in classical force fields (Table S1), making electrostatic interactions with Lewis bases and  $\pi$ -surfaces incorrectly unfavorable. Efforts are underway to modify conventional force fields to account for halogen bonding.<sup>52–55</sup> We believe that by demonstrating the reproduction of experimental data, our results could provide a platform to aid in the discovery of novel halogenated inhibitors and at the same time, offer optimism for the development of more accurate halogen-mapping strategies that incorporate modified force fields.

## ASSOCIATED CONTENT

### Supporting Information

Simulation setups and analysis procedures. Figures and table referred to in the paper. This material is available free of charge via the Internet at <http://pubs.acs.org>.

## AUTHOR INFORMATION

### Corresponding Author

\*E-mail: chandra@bii.a-star.edu.sg.

### Notes

The authors declare no competing financial interest.

## ACKNOWLEDGMENTS

We are grateful for funding from BMSI, Agency for Science, Technology and Research (Singapore). Y.S.T. was supported by an A\*STAR Graduate Scholarship.

## REFERENCES

- (1) Hernandes, M. Z.; Cavalcanti, S. M. T.; Moreira, D. R. M.; de Azevedo, W. F., Jr.; Lima Leite, A. C. Halogen atoms in the modern medicinal chemistry: hints for the drug design. *Curr. Drug Targets* **2010**, *11*, 303–314.
- (2) Gerebtzoff, G.; Li-Blatter, X.; Fischer, H.; Frentzel, A.; Seelig, A. Halogenation of drugs enhances membrane binding and permeation. *ChemBioChem* **2004**, *5*, 676–684.
- (3) Gentry, C. L.; Egletton, R. D.; Gillespie, T.; Abbruscato, T. J.; Bechowski, H. B.; Hruby, V. J.; Davis, T. P. The effect of halogenation on blood-brain barrier permeability of a novel peptide drug. *Peptides* **1999**, *20*, 1229–1238.
- (4) Metrangolo, P.; Resnati, G. Halogen bonding: a paradigm in supramolecular chemistry. *Chem.—Eur. J.* **2001**, *7*, 2511–2519.
- (5) Clark, T.; Hennemann, M.; Murray, J. S.; Politzer, P. Halogen bonding: the sigma-hole. *J. Mol. Model.* **2007**, *13*, 291–296.
- (6) Metrangolo, P.; Neukirch, H.; Pilati, T.; Resnati, G. Halogen bonding based recognition processes: a world parallel to hydrogen bonding. *Acc. Chem. Res.* **2005**, *38*, 386–395.
- (7) Wilcken, R.; Zimmermann, M. O.; Lange, A.; Joerger, A. C.; Boeckler, F. M. Principles and applications of halogen bonding in medicinal chemistry and chemical biology. *J. Med. Chem.* **2013**, *56*, 1363–1388.
- (8) Xu, Z.; Liu, Z.; Chen, T.; Chen, T.; Wang, Z.; Tian, G.; Shi, J.; Wang, X.; Lu, Y.; Yan, X.; Wang, G.; Jiang, H.; Chen, K.; Wang, S.; Xu, Y.; Shen, J.; Zhu, W. Utilization of halogen bond in lead optimization: a case study of rational design of potent phosphodiesterase type 5 (PDES) inhibitors. *J. Med. Chem.* **2011**, *54*, 5607–5611.
- (9) Hardegger, L. A.; Kuhn, B.; Spinnler, B.; Anselm, L.; Ecabert, R.; Stihle, M.; Gsell, B.; Thoma, R.; Diez, J.; Benz, J.; Plancher, J.-M.; Hartmann, G.; Banner, D. W.; Haap, W.; Diederich, F. Systematic investigation of halogen bonding in protein-ligand interactions. *Angew. Chem., Int. Ed.* **2011**, *50*, 314–318.
- (10) Rohde, L. A. H.; Ahring, P. K.; Jensen, M. L.; Nielsen, E. O.; Peters, D.; Helgstrand, C.; Krintel, C.; Harpsoe, K.; Gajhede, M.; Kastrup, J. S.; Balle, T. Intersubunit bridge formation governs agonist efficacy at nicotinic acetylcholine  $\alpha 4\beta 2$  receptors: unique role of halogen bonding revealed. *J. Biol. Chem.* **2012**, *287*, 4248–4259.
- (11) Mattos, C.; Ringe, D. Locating and characterizing binding sites on proteins. *Nat. Biotechnol.* **1996**, *14*, 595–599.
- (12) Goodford, P. J. A computational procedure for determining energetically favorable binding sites on biologically important macromolecules. *J. Med. Chem.* **1985**, *28*, 849–857.
- (13) Miranker, A.; Karplus, M. Functionality maps of binding sites: a multiple copy simultaneous search method. *Proteins* **1991**, *11*, 29–34.
- (14) Brenke, R.; Kozakov, D.; Chuang, G.-Y.; Beglov, D.; Hall, D.; Landon, M. R.; Mattos, C.; Vajda, S. Fragment-based identification of druggable ‘hot spots’ of proteins using Fourier domain correlation techniques. *Bioinformatics* **2009**, *25*, 621–627.

- (15) Ivetaç, A.; McCammon, J. A. Mapping the druggable allosteric space of G-protein coupled receptors: a fragment-based molecular dynamics approach. *Chem. Biol. Drug Des.* **2010**, *76*, 201–217.
- (16) Seco, J.; Luque, F. J.; Barril, X. Binding site detection and druggability index from first principles. *J. Med. Chem.* **2009**, *52*, 2363–2371.
- (17) Guvench, O.; MacKerell, A. D., Jr. Computational fragment-based binding site identification by ligand competitive saturation. *PLoS Comp. Biol.* **2009**, *5*, e1000435.
- (18) Lexa, K. W.; Carlson, H. A. Full protein flexibility is essential for proper hot-spot mapping. *J. Am. Chem. Soc.* **2011**, *133*, 200–202.
- (19) Bakan, A.; Nevins, N.; Lakdawala, A. S.; Bahar, I. Druggability assessment of allosteric proteins by dynamics simulations in the presence of probe molecules. *J. Chem. Theory Comput.* **2012**, *8*, 2435–2447.
- (20) Tan, Y. S.; Sledz, P.; Lang, S.; Stubbs, C. J.; Spring, D. R.; Abell, C.; Best, R. B. Using ligand-mapping simulations to design a ligand selectively targeting a cryptic surface pocket of polo-like kinase 1. *Angew. Chem., Int. Ed.* **2012**, *51*, 10078–10081.
- (21) Zhu, M.; De Simone, A.; Schenck, D.; Toth, G.; Dobson, C. M.; Vendruscolo, M. Identification of small-molecule binding pockets in the soluble monomeric form of the  $\text{A}\beta 42$  peptide. *J. Chem. Phys.* **2013**, *139*, 035101.
- (22) Basse, M. J.; Betzi, S.; Bourgeas, R.; Bouzidi, S.; Chetrit, B.; Hamon, V.; Morelli, X.; Roche, P. 2P21db: a structural database dedicated to orthosteric modulation of protein-protein interactions. *Nucleic Acids Res.* **2013**, *41*, D824–D827.
- (23) Xu, Z.; Yang, Z.; Liu, Y.; Lu, Y.; Chen, K.; Zhu, W. Halogen bond: its role beyond drug–target binding affinity for drug discovery and development. *J. Chem. Inf. Model.* **2014**, *54*, 69–78.
- (24) Foster, T. J.; Mackerell, A. D., Jr.; Guvench, O. Balancing target flexibility and target denaturation in computational fragment-based inhibitor discovery. *J. Comput. Chem.* **2012**, *33*, 1880–91.
- (25) Kussie, P. H.; Gorina, S.; Marechal, V.; Elenbaas, B.; Moreau, J.; Levine, A. J.; Pavletich, N. P. Structure of the MDM2 oncoprotein bound to the p53 tumor suppressor transactivation domain. *Science* **1996**, *274*, 948–953.
- (26) Grasberger, B. L.; Lu, T. B.; Schubert, C.; Parks, D. J.; Carver, T. E.; Koblish, H. K.; Cummings, M. D.; LaFrance, L. V.; Milkiewicz, K. L.; Calvo, R. R.; Maguire, D.; Lattanze, J.; Franks, C. F.; Zhao, S. Y.; Ramachandren, K.; Bylebyl, G. R.; Zhang, M.; Manthey, C. L.; Petrella, E. C.; Pantoliano, M. W.; Deckman, I. C.; Spurlino, J. C.; Maroney, A. C.; Tomczuk, B. E.; Molloy, C. J.; Bone, R. F. Discovery and cocrystal structure of benzodiazepinedione HDM2 antagonists that activate p53 in cells. *J. Med. Chem.* **2005**, *48*, 909–912.
- (27) Vassilev, L. T.; Vu, B. T.; Graves, B.; Carvajal, D.; Podlaski, F.; Filipovic, Z.; Kong, N.; Kammlott, U.; Lukacs, C.; Klein, C.; Fotouhi, N.; Liu, E. A. In vivo activation of the p53 pathway by small-molecule antagonists of MDM2. *Science* **2004**, *303*, 844–848.
- (28) Bista, M.; Wolf, S.; Khoury, K.; Kowalska, K.; Huang, Y.; Wrona, E.; Arciniega, M.; Popowicz, G. M.; Holak, T. A.; Domling, A. Transient protein states in designing inhibitors of the MDM2-p53 interaction. *Structure* **2013**, *21*, 2143–2151.
- (29) Baek, S.; Kutchukian, P. S.; Verdine, G. L.; Huber, R.; Holak, T. A.; Lee, K. W.; Popowicz, G. M. Structure of the stapled p53 peptide bound to Mdm2. *J. Am. Chem. Soc.* **2012**, *134*, 103–106.
- (30) Miyazaki, M.; Naito, H.; Sugimoto, Y.; Yoshida, K.; Kawato, H.; Okayama, T.; Shimizu, H.; Miyazaki, M.; Kitagawa, M.; Seki, T.; Fukutake, S.; Shiose, Y.; Aonuma, M.; Soga, T. Synthesis and evaluation of novel orally active p53-MDM2 interaction inhibitors. *Bioorg. Med. Chem.* **2013**, *21*, 4319–4331.
- (31) de Turiso, F. G.-L.; Sun, D.; Rew, Y.; Bartberger, M. D.; Beck, H. P.; Canon, J.; Chen, A.; Chow, D.; Correll, T. L.; Huang, X.; Julian, L. D.; Kayser, F.; Lo, M.-C.; Long, A. M.; McMinn, D.; Oliner, J. D.; Osgood, T.; Powers, J. P.; Saiki, A. Y.; Schneider, S.; Shaffer, P.; Xiao, S.-H.; Yakowec, P.; Yan, X.; Ye, Q.; Yu, D.; Zhao, X.; Zhou, J.; Medina, J. C.; Olson, S. H. Rational design and binding mode duality of MDM2-p53 inhibitors. *J. Med. Chem.* **2013**, *56*, 4053–4070.
- (32) Nelson, B. H.; Willerford, D. M., Biology of the interleukin-2 receptor. In *Advances in Immunology*, Dixon, F. J., Ed. 1998; Vol. 70, pp 1–81.
- (33) Arkin, M. R.; Randal, M.; DeLano, W. L.; Hyde, J.; Luong, T. N.; Oslob, J. D.; Raphael, D. R.; Taylor, L.; Wang, J.; McDowell, R. S.; Wells, J. A.; Braisted, A. C. Binding of small molecules to an adaptive protein-protein interface. *Proc. Natl. Acad. Sci. U. S. A.* **2003**, *100*, 1603–1608.
- (34) Braisted, A. C.; Oslob, J. D.; Delano, W. L.; Hyde, J.; McDowell, R. S.; Waal, N.; Yu, C.; Arkin, M. R.; Raimundo, B. C. Discovery of a potent small molecule IL-2 inhibitor through fragment assembly. *J. Am. Chem. Soc.* **2003**, *125*, 3714–3715.
- (35) Thanos, C. D.; Randal, M.; Wells, J. A. Potent small-molecule binding to a dynamic hot spot on IL-2. *J. Am. Chem. Soc.* **2003**, *125*, 15280–15281.
- (36) Thanos, C. D.; DeLano, W. L.; Wells, J. A. Hot-spot mimicry of a cytokine receptor by a small molecule. *Proc. Natl. Acad. Sci. U. S. A.* **2006**, *103*, 15422–15427.
- (37) Adams, J. M. Ways of dying: multiple pathways to apoptosis. *Genes Dev.* **2003**, *17*, 2481–2495.
- (38) Wuilleme-Toumi, S.; Robillard, N.; Gomez, P.; Moreau, P.; Le Gouill, S.; Avet-Loiseau, H.; Harousseau, J. L.; Amiot, M.; Bataille, R. Mcl-1 is overexpressed in multiple myeloma and associated with relapse and shorter survival. *Leukemia* **2005**, *19*, 1248–1252.
- (39) Boisvert-Adamo, K.; Longmate, W.; Abel, E. V.; Aplin, A. E. Mcl-1 Is Required for Melanoma Cell Resistance to Anoikis. *Mol. Cancer Res.* **2009**, *7*, 549–556.
- (40) Ding, Q.; He, X.; Xia, W.; Hsu, J.-M.; Chen, C.-T.; Li, L.-Y.; Lee, D.-F.; Yang, J.-Y.; Xie, X.; Liu, J.-C.; Hung, M.-C. Myeloid cell leukemia-1 inversely correlates with glycogen synthase kinase-3 $\beta$  activity and associates with poor prognosis in human breast cancer. *Cancer Res.* **2007**, *67*, 4564–4571.
- (41) Lessene, G.; Czabotar, P. E.; Colman, P. M. BCL-2 family antagonists for cancer therapy. *Nat. Rev. Drug Discovery* **2008**, *7*, 989–1000.
- (42) Friberg, A.; Vigil, D.; Zhao, B.; Daniels, R. N.; Burke, J. P.; Garcia-Barrantes, P. M.; Camper, D.; Chauder, B. A.; Lee, T.; Olejniczak, E. T.; Fesik, S. W. Discovery of potent myeloid cell leukemia 1 (Mcl-1) inhibitors using fragment-based methods and structure-based design. *J. Med. Chem.* **2013**, *56*, 15–30.
- (43) Tanaka, Y.; Aikawa, K.; Nishida, G.; Homma, M.; Sogabe, S.; Igaki, S.; Hayano, Y.; Sameshima, T.; Miyahisa, I.; Kawamoto, T.; Tawada, M.; Imai, Y.; Inazuka, M.; Cho, N.; Imaeda, Y.; Ishikawa, T. Discovery of potent Mcl-1/Bcl-xL dual inhibitors by using a hybridization strategy based on structural analysis of target proteins. *J. Med. Chem.* **2013**, *56*, 9635–9645.
- (44) Labi, V.; Erlacher, M.; Kiessling, S.; Villunger, A. BH3-only proteins in cell death initiation, malignant disease and anticancer therapy. *Cell Death Differ.* **2006**, *13*, 1325–1338.
- (45) Amundson, S. A.; Myers, T. G.; Scudiero, D.; Kitada, S.; Reed, J. C.; Fornace, A. J. An informatics approach identifying markers of chemosensitivity in human cancer cell lines. *Cancer Res.* **2000**, *60*, 6101–6110.
- (46) Muchmore, S. W.; Sattler, M.; Liang, H.; Meadows, R. P.; Harlan, J. E.; Yoon, H. S.; Nettesheim, D.; Chang, B. S.; Thompson, C. B.; Wong, S. L.; Ng, S. C.; Fesik, S. W. X-ray and NMR structure of human Bcl-x(L), an inhibitor of programmed cell death. *Nature* **1996**, *381*, 335–341.
- (47) Manion, M. K.; O'Neill, J. W.; Giedt, C. D.; Kim, K. M.; Zhang, K. Y. Z.; Hockenberry, D. M. Bcl-X-L mutations suppress cellular sensitivity to antimycin A. *J. Biol. Chem.* **2004**, *279*, 2159–2165.
- (48) Wysoczanski, P.; Mart, R. J.; Loveridge, E. J.; Williams, C.; Whittaker, S. B. M.; Crump, M. P.; Allemann, R. K. NMR solution structure of a photoswitchable apoptosis activating Bak peptide bound to Bcl-x(L). *J. Am. Chem. Soc.* **2012**, *134*, 7644–7647.
- (49) Brady, R. M.; Vom, A.; Roy, M. J.; Toovey, N.; Smith, B. J.; Moss, R. M.; Hatzis, E.; Huang, D. C. S.; Parisot, J. P.; Yang, H.; Street, I. P.; Colman, P. M.; Czabotar, P. E.; Baell, J. B.; Lessene, G. De-novo designed library of benzoylureas as inhibitors of BCL-XL:

- synthesis, structural and biochemical characterization. *J. Med. Chem.* **2014**, *57*, 1323–1343.
- (50) Stauber, D. J.; Debler, E. W.; Horton, P. A.; Smith, K. A.; Wilson, I. A. Crystal structure of the IL-2 signaling complex: paradigm for a heterotrimeric cytokine receptor. *Proc. Natl. Acad. Sci. U. S. A.* **2006**, *103*, 2788–2793.
- (51) Wang, J. M.; Wolf, R. M.; Caldwell, J. W.; Kollman, P. A.; Case, D. A. Development and testing of a general amber force field. *J. Comput. Chem.* **2004**, *25*, 1157–1174.
- (52) Ibrahim, M. A. A Molecular mechanical study of halogen bonding in drug discovery. *J. Comput. Chem.* **2011**, *32*, 2564–2574.
- (53) Rendine, S.; Pieraccini, S.; Forni, A.; Sironi, M. Halogen bonding in ligand-receptor systems in the framework of classical force fields. *Phys. Chem. Chem. Phys.* **2011**, *13*, 19508–19516.
- (54) Jorgensen, W. L.; Schyman, P. Treatment of halogen bonding in the OPLS-AA force field: application to potent anti-HIV agents. *J. Chem. Theory Comput.* **2012**, *8*, 3895–3901.
- (55) Du, L.; Gao, J.; Bi, F.; Wang, L.; Liu, C. A polarizable ellipsoidal force field for halogen bonds. *J. Comput. Chem.* **2013**, *34*, 2032–2040.